A Lattice Monte Carlo Study of Long Chain Conformations at Solid–Polymer Melt Interfaces

ARTICLE *in* THE JOURNAL OF CHEMICAL PHYSICS · AUGUST 1993

Impact Factor: 2.95 · DOI: 10.1063/1.465163 · Source: OAI

2 AUTHORS:

Ioannis Bitsanis
Foundation for Research and Technology…
48 PUBLICATIONS **1,254** CITATIONS

SEE PROFILE

G. ten Brinke
University of Groningen
280 PUBLICATIONS **9,409** CITATIONS

SEE PROFILE

A lattice Monte Carlo study of long chain conformations at solid–polymer melt interfaces

Ioannis A. Bitsanis[a)]
Department of Chemical Engineering, University of Florida, Gainesville, Florida 32611

Gerrit ten Brinke
Department of Chemistry, University of Groningen, Nijeborgh 16, 9747 AG, Groningen, The Netherlands

(Received 23 March 1993; accepted 3 May 1993)

In this paper we present a comprehensive lattice Monte Carlo study of long chain conformations at solid–polymer melt interfaces. Segmental scale interfacial features, like the bond orientational distribution were found to be independent of surface–segment energetics, and statistically identical with Helfand's predictions for the full-occupancy, infinite chain length limit. Conformational statistics of chains longer than 5–6 *statistical* segments followed the predictions of the Scheutjens–Fleer theory and the same power laws as a single ideal chain at the critical value of the surface–segment adsorption free-energy. Our simulations tested the predictions of random walk next to a "reflective" surface statistics for the spatial variations of chain dimensions and chain center of mass density. It was found that these statistics furnish the correct long chain limit, independently of surface–segment energetics. The random walk next to a "reflective" boundary predictions for the "adsorbed" amount and the distributions of tail, loop, and train number, as well as tail and loop size were in quantitative agreement with the simulation data. The correspondence between random walks and real (or simulated) chains required the knowledge of a single, microscopic parameter, the number of chemical segments per statistical segment, a_∞. This quantity was very close to the average length of adsorbed sequences (trains), in the long chain limit. Our simulations tested thoroughly and established firmly the validity of "reflective" boundary statistics in the melt. The inevitability of these statistics has broad implications on "desorption" kinetics, chain mobility, and chain relaxation, which are currently under study.

I. INTRODUCTION

Understanding molecular structure—thermodynamics, and microscopic dynamics—rheology of polymeric melts next to solid surfaces is essential in thin film lubrication, adhesion, and polymer processing. As a result of the general trend towards miniaturization, technological applications frequently process, use, or manufacture polymer films so thin that their properties differ greatly from the bulk properties of the same material. Under these circumstances, it is necessary to understand thermodynamics and rheology at a molecular level.

Solid–homopolymer melt interfaces have been studied mostly as a limiting case of solid–homopolymer solution interfaces. Early theories[1,2] contained certain drastic and probably unwarranted assumptions. The first comprehensive theory of solid–homopolymer solution interfaces was developed by Roe.[3] Roe's theory was later criticized[4,5] because it contained the assumption of identical density profiles for all segments, regardless of their position along the chain, as well as its handling of the inversion symmetry for chain conformations. Helfand[4] developed a lattice model for solid–polymer solution interfaces. Brief consideration was given to the solid–homopolymer melt interface in the infinite molecular weight, incompressible limit. This work contains an excellent discussion of surface-induced bond anisotropy and the mechanism for gradual relief of the associated loss of conformational entropy.

An elegant "matrix method" was introduced by Di Marzio and Rubin[5] and was employed for the study of a polymer confined between two plates. Scheutjens and Fleer[6] modified this method and employed it in the most detailed study of homopolymer adsorption to date. Their calculations of finite molecular weight solutions, spanned the whole concentration range from extremely dilute solutions to incompressible melts. Of particular relevance to our work was their study of chain conformations and distribution of chain segments in trains, loops, and tails. Theodorou[7] applied a variant of the Scheutjens–Fleer theory to solid–homopolymer and solid–block-copolymer melt interfaces. He studied the molecular weight dependence of the surface free energy and finite compressibility effects. In the infinite molecular weight, incompressible limit his results agreed with Helfand's.[4] Theodorou's calculations predicted a very weak and diminishing molecular weight dependence of the interfacial structure.

Silberberg[8] adopted an ad hoc approach allowing direct use of several results from the theory of random walks (Feller[9]). He introduced a set of principles for "conformation transfer," which involve "segmental swapping" between unconstrained chains. The solid surface is replaced by an imaginary penetrable plane cutting through the bulk melt. Each chain (conformation) is labeled by its "start," which is identified as the chain end closest to the

a)Author to whom correspondence should be addressed.

 0021-9606/93/99(4)/3100/12/$6.00

imaginary plane. The chain is then assigned to the half-space containing its "start," and its segments belonging to the other half-space are swapped between the chain and its mirror image. This procedure leads to two segregated groups of chains, each containing chains, that lie entirely in the upper or lower half space. The treatment has its roots to the "single ideal chain next to a barrier" problem, which was solved during the 1960s.[10–13]

The use of Silberberg's procedure as a tool for counting chain conformations makes good physical sense. The adopted set of rules preserves the number of one-chain conformations, as conformations are always "reflected," never eliminated ("adsorbed"). Thus, it reproduces the dominant feature of a solid–(incompressible) melt interface, constant density on a scale coarser than the statistical segment size.

This set of rules is mathematically equivalent to the application of a "reflective" boundary condition[14] in the "diffusion equation" describing one chain statistics in the bulk melt. Consistency with the modeling of chains as Gaussian coils requires that the "reflective" boundary condition be applied to statistical, rather than actual, segments. However, the statistical segment inside the interface cannot be identical with the bulk. This difficulty serves as a reminder of the ad hoc nature of Silberberg's approach. Properties whose prediction depends critically on an accurate representation of interfacial structure (e.g., excess surface free energy) require more rigorous theories.[3–7]

The theoretical approaches discussed above supply two types of information (i) coarse grained (over one segment, size) density and bond orientation profiles needed for surface tension or excess surface free energy calculations; and (ii) large scale features of chain conformations.[6,8]

The second type of information constitutes the structural basis for the analysis of long chain mobility and relaxation. The solid–incompressible melt interface is rather unique in this respect. Chain conformational statistics must be universal in the strongest sense, i.e., independent of chain intramolecular architecture, molecular weight *and* strength of surface–segment interaction, since the statistical weight of any microscopic conformation of the many-chain system is not affected by surface–segment energetics[4] (in the full-occupancy limit).

In this paper we present a molecular simulation study of chain conformational statistics at solid–melt interfaces. Our simulations span a wide range of chain lengths, from well below (5-mers) to well inside (300-mers) the scaling regime. We focus on testing relevant theoretical predictions and Silberberg's approach of segmental swap between unconstrained mirror image conformations,[8] in particular. The close relation of this approach with simple random walk statistics,[9] makes the prospect of its use as a structural basis for the analysis of chain dynamics very appealing. The universality of chain conformations at solid–melt interfaces underscores the value of analytical predictions resulting from the "reflective boundary" approach.[8] A by-product of our work is a molecular simulation demonstration of the very minor importance of finite molecular weight and compressibility effects on segmental scale structural features (interfacial density and bond orientation profiles) at melt densities, well in agreement with theoretical predictions[3,4,6,7] and considerably more limited earlier simulation results.[15–17]

Earlier simulation studies[15–21] concentrated on segmental scale interfacial features, where they supplied a wealth of information. Chain conformations were studied to a much lesser extent, and no systematic comparison with available theoretical predictions was presented. Certain conclusions drawn from these earlier studies reflected short chain effects, which disappear in the long chain limit.

We consider this paper as a prelude to a broad study of chain dynamics. This future goal has biased our focus in favor of conformational features, which are expected to have a significant effect on chain dynamics. Despite earlier attempts,[16,18] such a study is still needed. Past simulation studies enhanced considerably our understanding of dynamics at solid–melt interfaces. Nevertheless, they were limited to short chainlengths and rather mild surface–segment energetics. These factors may be responsible for the profound discrepancies between simulation and experimental findings.[22–24]

The rest of this paper has been organized as follows: Sec. II describes briefly the simulation technique. Sections III, IV, and V contain our simulation findings. More specifically, Sec. III discusses briefly a few segmental scale interfacial features, Sec. IV compares our simulation findings with Silberberg's "reflective boundary" predictions,[8] and Sec. V extends these comparisons to features like trains, loops, and tails of the adsorbed chains. Finally, Sec. VI summarizes our results and discusses some of their implications.

II. THE SIMULATION TECHNIQUE

In order to simulate melts of long polymer chains confined between parallel plates we employed a lattice Monte Carlo simulation technique very similar to that used in Ref. 15. Lattice Monte Carlo simulations have a long history in polymer physics. Like all simulation methods, they represent a compromise between the desire for detailed molecular modeling and the need for computational efficiency. Lattice simulations in particular, cannot reveal any subtle subsegmental scale features like those observed in continuous simulations.[17–21] Therefore, they supply less detailed information on the variation of structural features (density, bond orientation, end segment density) inside the narrow solid–melt interface. Continuous and lattice simulation results agree with each other, when the continuous profiles are coarse-grained over one segment diameter[15,17,18] (for comparable lattice and continuous models).

Lattice simulations are entirely appropriate for the modeling of large scale conformational features of long chains. Since this is the type of information sought in this study, the considerable computational advantage of lattice over continuous simulations singled them out as the preferred type of modeling. Furthermore, lattice simulations facilitate the comparison with relevant theoretical predictions.[4,6–8]

In what follows we describe briefly the simulation method. A more detailed exposition can be found in Ref. 15. A cubic lattice was used because of its simplicity in the handling of adsorption problems. The two impenetrable solid surfaces were placed at $z=1$ and $z=h$. Periodic boundary conditions were applied in the x and y directions with the periodic boundaries located at $x=1$, $x=s$, and $y=1$, $y=s$.

The simulation method is a combination of the procedure introduced by Kolinski *et al.*[25] for simultaneous growth and equilibration of chains, with the elementary bead motions of Kovac *et al.*[26] Initially, the chain "heads" are placed randomly on the lattice and chain growth proceeds by adding randomly one segment to either end of a randomly selected chain. When a chain has reached a prescribed short length (this was chosen as five segments in our simulations) growth and equilibration start to compete. Equilibration consists of a reptation step[27] and a segment jump attempt. The possible jumps are different for end and middle segments. End segments may flip by 90°, while middle segments can undergo a "normal" jump or a "crankshaft" motion, as introduced by Lax and Brender.[28] If one intends to study time correlation functions and is concerned about the reproduction of proper (Rouse) microscopic dynamics the reptation step should not be used.[25] The use of a reptation step, however, does not affect static properties, and it speeds up equilibration considerably.[27]

Energetics were very simple in our simulations. Excluded volume interactions were taken into account by rejecting movements that resulted in multiple occupancy of lattice sites. Cohesive forces between segments were ignored, since they are known to have little effect on large scale conformational features (the Lennard-Jones energy parameter for methyl–methyl interactions is $\sim 0.2kT$ at room temperature). ϵ, the only energy parameter used, specified the strength of the solid–segment potential, i.e., segments at $z=1$ and $z=h$ experienced an attractive potential equal to $-\epsilon/kT$. Chain conformations depend very sensitively on ϵ at *low volume fractions*. The effect of solid–segment attraction is expected to be very weak at the high densities typical of melts. This effect vanishes altogether on a fully occupied lattice (incompressible melt).[4]

Volume fractions of ~ 0.8 were used in all simulations. This is somewhat lower than a typical melt density at room temperature. Technical information on the simulation runs is summarized in Table I.

TABLE I. Simulation parameters.

Chain length (N)	Surface–segment energy (ϵ)	Film thickness (h)	Number of chains	Size of periodic box	Number of MC moves ($\times 10^6$)
5	0.0	18	192	8	8.0
5	1.0	18	198	8	8.0
10	0.0	18	96	8	10.0
10	1.0	18	99	8	15.0
20	0.0	20	54	8	20.0
20	1.0	21	57	8	20.0
30	0.0	30	53	8	40.0
30	1.0	28	50	8	40.0
50	0.0	50	117	12	100.0
50	1.0	49	116	12	100.0
100	0.0	59	94	14	200.0
200	0.0	59	69	17	300.0
300	0.0	59	64	20	300.0
300	0.0	59	100	25	300.0

III. SEGMENTAL SCALE FEATURES

Although our main goal is to study large scale conformational features of melt chains in molecular proximity with a planar solid surface, we present here some of our results on the structural features inside the narrow (~ 2 lattice spacings) solid–melt interface. This discussion will put the subsequent presentation of large scale conformational features in context, as its main purpose is to demonstrate the insensitivity of segmental scale interfacial structure on chainlength, finite compressibility and surface-segment adsorption energy.

The effect of chain length on the density profiles of high density melts ($\rho=0.8$) next to a neutral solid surface ($\epsilon=0.0$) is shown in Fig. 1(a). The comparison of the density profiles for three different surfaces ($\epsilon=0.0$, 0.5, 1.0) is shown in Fig. 1b. All these profiles were determined from simulations of wide melt films with the effects of the two surfaces being clearly separable. Furthermore, all profiles were symmetrized over the two surfaces. The profiles

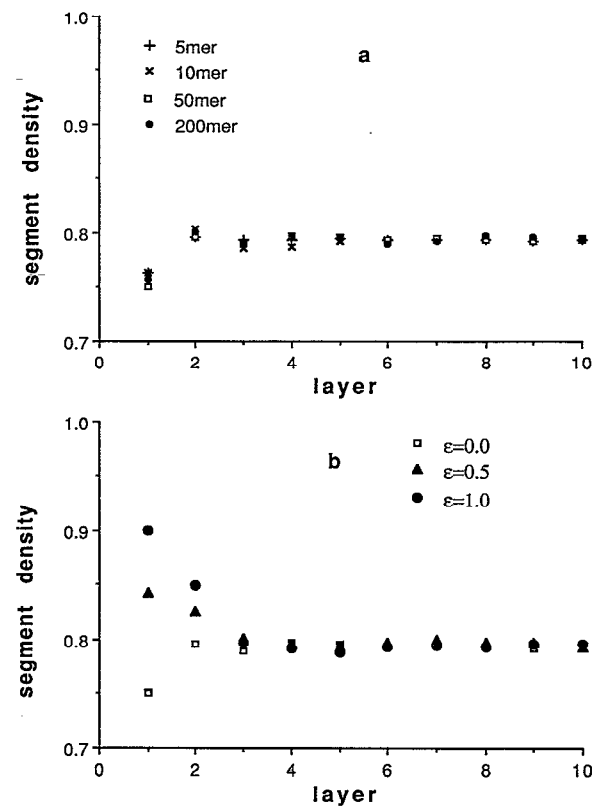

FIG. 1. (a) Segment density profiles for various chain lengths ($\epsilon=0.0$). (b) Segment density profiles for various surface–segment energies ($N=50$).

in Fig. 1(a) are identical to within the noise level (0.005–0.01). This shows that most of the transient effect towards a chain length independent density pattern[18] occurs on a subsegmental scale. Chains of different lengths consisting of just a few statistical segments (as we shall discuss later one statistical segment corresponds to 1.8 actual segments of our model) develop identical density profiles on a scale coarser than one segment diameter.

The effect of surface attraction is quantified in Fig. 1(b). Comparable density profiles correspond to melt films confined between different surfaces but being at equilibrium with the same bulk reservoir (a bulk melt with occupancy of 0.8), i.e., having the same chemical potential. Efficient techniques for constant chemical potential Monte Carlo simulations of fluids consisting of chain molecules are currently under development.[29–31] In this work we adopted a much simpler approach based on the "superposition approximation,"[32] which is known to be quite accurate for wide films with well-separated interfaces.[33,34]

As we can see from Fig. 1(b), the interfacial density variations are short range (two lattice spacings) for all three surfaces. This is a direct consequence of the very short static screening length in the melt. The extent of the surface attraction effect, which is null on a fully occupied lattice, is a measure of our systems' proximity to the incompressible melt limit. Again, we are witnessing the predominance of packing considerations in shaping the interfacial structure of dense liquids. The shortage of available "free volume" limits density variations to a low level, which allows their screening within a couple of segment (or one statistical segment) sizes.

The lack of any interfacial density variations in the case of an incompressible melt does not imply the absence of spatial variations in other structural features. The presence of the solid surface perturbs the spherical symmetry of the bond orientational distribution. This phenomenon is most conveniently analyzed in terms of the "bond anisotropy factors" g_l^v introduced by Helfand.[4] g_l^v is the ratio of the probability of a bond emanating from the lth layer to step in the v-direction, over the same probability in a bulk system. For a cubic lattice

$$v = \begin{matrix} - \text{bonds stepping towards the surface} \\ 0 \text{ bonds stepping parallel to the surface} \\ + \text{bonds stepping away from the surface.} \end{matrix} \qquad (3.1)$$

Obviously, $g_l^v = 1$ in the bulk, and $g_{l+1}^- = g_l^+$ because the chain cannot distinguish "head" and "tail."

Bond anisotropy profiles for an infinite molecular weight melt on a fully occupied cubic lattice next to a planar surface were calculated using Helfand's lattice model.[4] They were predicted to become practically isotropic after the second layer (differed from the bulk value of 1.00 by <0.01). Finite molecular weight effects on the bond orientational distribution were calculated by Theodorou.[7] Even for 10-mers, bond anisotropy factors were predicted to differ by <0.02 from their infinite molecular weight asymptotic values. Our simulation data in Table II confirm the lack of any chain length, or adsorption strength dependence of the orientational bond distribution to within the statistical noise (0.02). The simulation results for the anisotropy factors of the first two layers are identical with Helfand's predictions,[4] despite the finite molecular weight and compressibility of our systems. Our results on the structural features of the interface (segment density and bond orientation profiles) attest to the theoretically predicted very weak dependence of these features on the adsorption energy parameter, at the high density of 0.8. Essentially, the only effect of ϵ is to increase slightly the density in the first layer. This increase must be small at realistic melt densities, and it is bound to vanish on a fully occupied lattice. Furthermore, "higher order" effects, like the molecular weight dependence of the density profile and bond orientational distribution, as well as the finite compressibility effect on the bond orientational distribution are found to be quantitatively insignificant.

TABLE II. First and second layer bond anisotropy factors [Eq. (3.1)].

Chain length (N)	Surface–segment energy (ϵ)	g_1^0	g_1^+	g_2^0	g_2^+
5	0.0	1.22	1.12	0.98	1.00
10	0.0	1.22	1.13	1.00	0.99
20	0.0	1.22	1.11	1.01	1.00
50	0.0	1.22	1.10	0.98	1.01
50	0.5	1.22	1.11	0.98	0.99
50	1.0	1.23	1.08	0.98	1.00
100	0.0	1.22	1.12	0.99	0.98
200	0.0	1.22	1.13	0.99	0.99
300	0.0	1.22	1.11	0.98	1.01
		Helfand's model (Ref. 4)			
∞	n/a	1.2262	1.0954	0.9786	0.9903

In short, the interfaces of all systems simulated are remarkably similar, and their features are very close to the infinite molecular weight, zero compressibility limit. At this limit the adsorption strength has no influence on the structural properties of the interface and on chain conformations. Close enough to this limit, as in our systems, the effect of ϵ on the structural features of the interface is found to be very weak.

IV. TEST OF THE "REFLECTIVE BOUNDARY" APPROACH

In this section we present our simulation results on a number of chain conformational features and compare them with predictions from Silberberg's "reflective boundary" approach.[8]

The physical content of these results will become clearer if we digress briefly on the relation between our model chains and random walks. Real polymer molecules in the melt and model chains in melt simulations behave, on an appropriate scale, like random walks. In particular, their radius of gyration (R_g) and their end-to-end distance (R) are expected to depend on the number of repeating units (N) in the following manner:

$$R_g^2 = \frac{1}{6}\frac{N^2-1}{N} c_1 b^2, \qquad (4.1a)$$

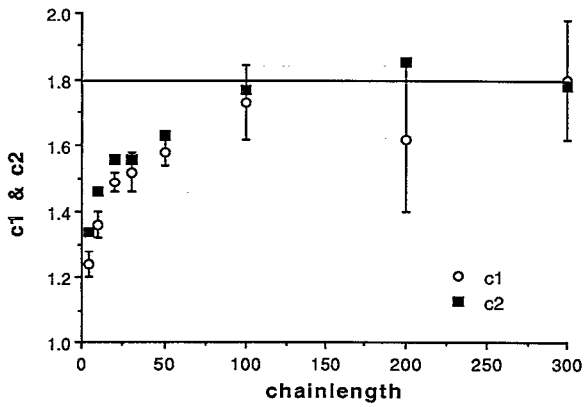

FIG. 2. The factors c_1 and c_2 [Eqs. (4.1a) and (4.1b)] for chains with their center of mass in the middle bulklike region of the films simulated.

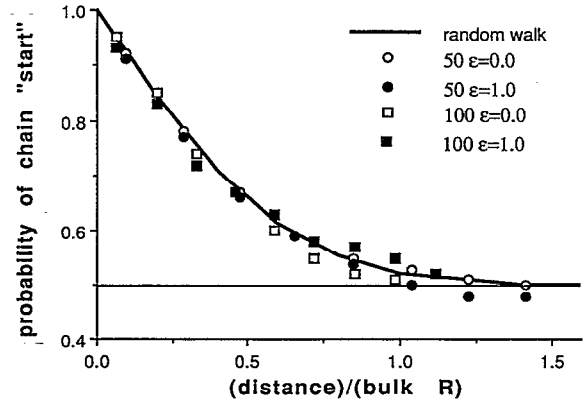

FIG. 3. Chain "start" profiles, i.e., the probability that a chain end found at a particular distance from the surface is a chain "start." A chain "start" is defined as the chain end closest to the surface.

$$R^2=(N-1)c_2b^2. \tag{4.1b}$$

In Eqs. (4.1), b is the size of the repeating unit (bond length) and c_1, c_2 are factors depending on intramolecular architecture *and* on chain length. For sufficiently long chains c_1 and c_2 become identical and chain length independent. Their common asymptotic value is usually designated by c_∞.

The approach of c_1 and c_2 to a common limit is shown in Fig. 2, which depicts our simulation results for chains in the middle of the wide films simulated. The centers of mass of these chains were located at a distance greater than three bulk end-to-end distances from the solid surfaces. c_∞ is found to be ~ 1.8 for our model chains on a cubic lattice. The exponents for R and R_g vs N, that fit our long chain data ($N>50$), were found to be 0.52 and 0.51, respectively.

Our data on c_1 and c_2 agree closely with more limited findings from earlier simulation studies.[15,35] The c_1 values in Ref. 15 and this work are identical for the chain length simulated in both studies (1.60 for $N=60$). Furthermore, after accounting for the density dependence of c_∞, ($c_\infty \approx \phi^{-0.25}$), our value for $c_\infty(1.8)$ is very close to the value from the continuous simulations of Kremer and Grest (1.77).[35] In fact the continuous "necklace" model used in Refs. 18 and 35 and the cubic lattice model in Ref. 15 and this work are very similar in several other respects, as well.[18]

It is often useful to relate long chains in the melt with random walks of a renormalized step size equal to $c_\infty^{1/2}b$. This new elementary entity, the Kuhn segment, represents a small group of chemical segments. A precise answer to the usual question, how many chemical segments are contained in a Kuhn (or statistical) segment, is very difficult. Good estimates however, are feasible, especially for model chains like these in our simulations. Few (<4) successive segment complexes of a self-avoiding random walk can be easily enumerated. If each configuration of these 3 segment complexes is assigned an equal probability (no segment–segment energetics), one finds that a 1.8 segment–complex will have, on the average, an end-to-end distance equal to $c_\infty^{1/2}b$. In other words, our estimate is that the statistical segment of our chains contains 1.8 actual segments.

The conformations assumed by chains in our simulations will be compared with those of *three-dimensional* random walks, unrestricted in two directions (x and y) and facing a "reflective boundary" in the third direction (z). Since the z-coordinate of the first lattice layer is 1 and the lattice spacing is also 1 the "reflective boundary" must be placed at $z=0.5$. Naturally, our simulations did not mimic a semi-infinite medium but a film of finite thickness. Therefore, we could have compared our simulation data with available predictions pertaining to random walks confined between two "reflective boundaries."[36,37] However, this was unnecessary, as effects resulting from the interference between the two surfaces were undetectable to within the noise level of our data. The elimination of interference effects was achieved at the expense of simulating quite wide films (around 20 bulk radii of gyration for $N<100$ and around 15 for $N\geqslant 100$). Despite its considerable computational cost, eliminating such effects was essential for our ongoing studies of chain dynamics.[38]

We start with a comparison, which tests very sensitively the validity of the "random walk next to a reflective boundary" statistics in reproducing actual chain conformations at solid–melt interfaces. Figure 3 compares our simulation data for the chain "start" probability with the corresponding "reflective boundary" prediction. A chain "start" is defined as the chain end closest to the surface. The quantity plotted in Fig. 3 is the probability that a chain end located at a distance z^* from the surface is a chain "start." This quantity varies between 1.0 (at the surface) and 0.5 (in the bulk). The data for a number of chain lengths and surface–segment energies collapse on the "random walk next to a reflective boundary" prediction.[8] This prediction is $1.0-(1/2)\mathrm{erf}(z^*/2^{1/2}R_z)$, where z^* is the distance of the chain end from the surface and R_z is the bulk end-to-end distance in one direction.

We continue with the profiles for chain centers of mass. Reflection of configurations leads to an accumulation of chain centers of mass at a distance equal to

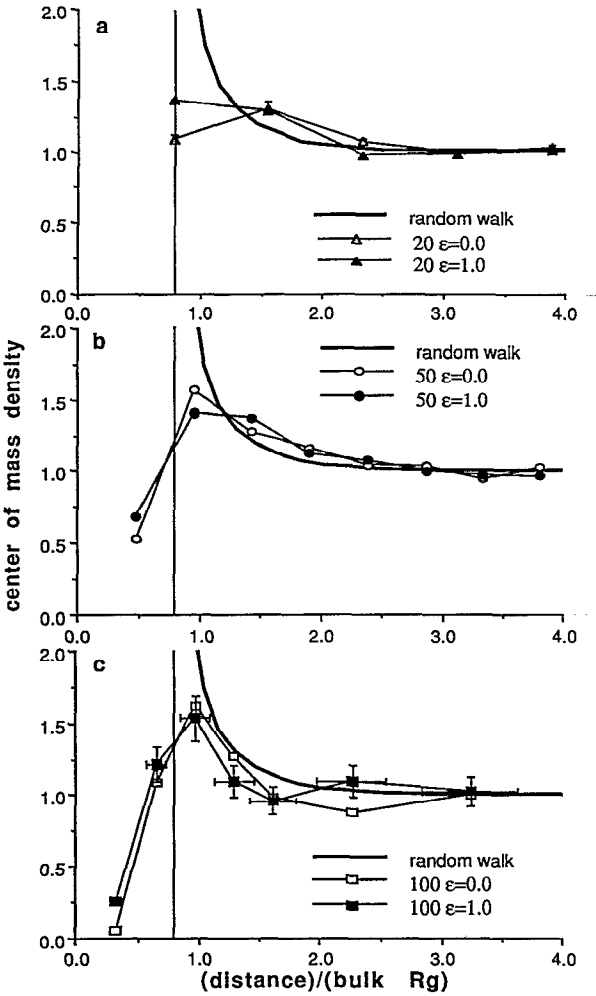

FIG. 4. Chain center of mass profiles (a) $N=20$; (b) $N=50$; (c) $N=100$.

$$z_0=(2/\pi)^{1/2}R_{gz}, \tag{4.2}$$

where, R_{gz} is the bulk radius of gyration in one-dimension. In fact, the chain center of mass profile resulting from a (continuous) random walk next to a reflective boundary diverges at this distance.[8] In real and simulated melts this divergence is avoided by the breakdown of the random flight description on a segmental scale. The center of mass density increases, in agreement with the "reflective boundary" prediction, until the segmental excluded volume effects take over and force a sharp depletion. Note that this depletion occurs at about one segment diameter from the surface. The placement of chain centers of mass even closer to the surface would require squeezing the hard core of segment–surface intermolecular forces.

The essence of the "reflective boundary" prediction as a useful limit is supported clearly by the comparisons presented in Figs. 4(a), 4(b), and 4(c). The divergence is smoothed out into a peak, which sharpens with chain length and broadens with surface–segment attraction. Our data indicate that the maximum of the profile will grow without bound with increasing chain length, and the divergence will be avoided by an ever sharper depletion inside a

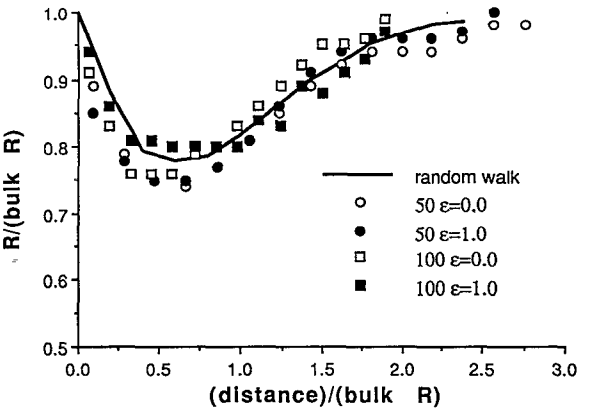

FIG. 5. Chain end to end distance normal to the surface vs position of chain "start." The distance in this and some subsequent figures is normalized by R, the *bulk* end-to-end distance in *one dimension*.

segmental scale region (the sharpening will result from our scaling of distances with the bulk radius of gyration).

Two comments are in order at this point. First, the peak is pushed away from the surface and broadened for short chains [Fig. 4(a)] because of the competition between segmental scale requirements (packing) and long chain conformational needs ("reflective boundary" statistics). The former dominate in the case of oligomers ($N=20$), while the latter prevail for long chains ($N=100$). Second, the effect of surface–segment attraction is to smooth out the peak of chain centers of mass [Figs. 4(a) and 4(b)], as it acts against the preservation of a constant segment density. This effect becomes dominant for very short chains, where the peak might even disappear [Fig. 4(a)]. However, the effect of surface–segment energetics is bound to vanish for sufficiently long chains at the high densities used in our simulations. The data for $N=100$ and $\epsilon=0.0$ and 1.0 attest to the surface-independent nature of long chain conformations at solid–melt interfaces [Fig. 4(c)].

An interesting consequence of "reflective boundary" statistics is the shrinking of chains in the direction normal to the surface. Indeed, reflection of conformations can only decrease the end-to-end distance normal to the surface.[8] This is the opposite of "absorbing boundary" statistics, where the elimination of conformations penetrating the boundary favors large end-to-end distances normal to the surface.[8,14] Figure 5 is a test of this prediction against our simulation data for two chain lengths ($N=50$ and 100) and two different surface–segment energies ($\epsilon=0.0$ and 1.0). The molecular weight and surface–segment energy independence of the end to end distance normal to the surface, as well as the quantitative agreement with the prediction of Ref. 8 is clearly demonstrated in Fig. 5.

The shrinking of chains in the direction normal to the surface had also been observed in a number of earlier simulation studies.[15–18] However, its origin was not understood clearly in these works, as it was attributed to segment layering, which (presumably) lead to the adoption of flat chain conformations. The comparison presented in Fig. 5

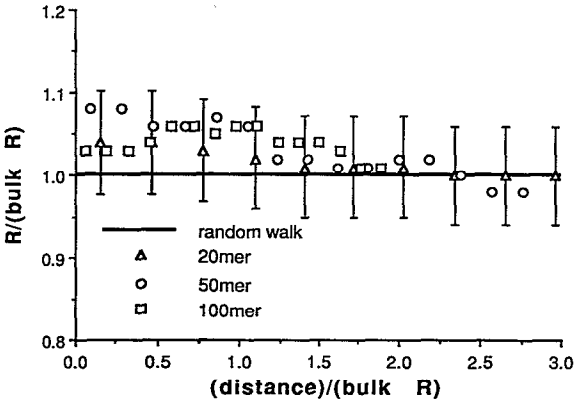

FIG. 6. Chain end-to-end distance parallel to the surface vs position of chain "start."

demonstrates that the effect is generic to random walk statistics next to a "reflective boundary," as its quantitative manifestation is in agreement with that predicted by the aforementioned statistics.

More direct evidence in favor of the above arguments is presented in Fig. 6. This figure depicts the variation of the end-to-end distance parallel to the surface, as a function of the location of chain "start" (closest to the surface chain end). If "flat" chain conformations were the rule, one would expect this quantity to increase close to the surface. Only a very slight increase is observed, which seems to diminish with chain length. The noise level of our data does not allow any quantitative study of this transient effect.

It is a direct consequence of random walk statistics next to a "reflective boundary" that two-dimensional chain conformations have a vanishingly small statistical weight in the long chain limit. The data shown in Figs. 2–6 demonstrate that chains at a solid–melt interface follow these statistics, regardless of surface–segment energetics. Therefore, it is no surprise that very few "two-dimensional" chains (none in the long chain limit) can be found at the solid–melt interface. This is depicted in Fig. 7, where the

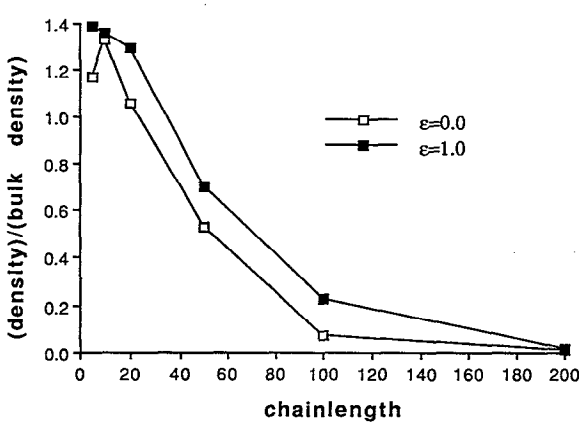

FIG. 7. Number of chains with their centers of mass between the first and second layers divided by the number of chains in the bulk with their centers of mass inside a slice of equal width (1 lattice spacing).

TABLE III. Notation on trains, loops, and tails.

	Train	Loop	Tail
Average number of per adsorbed chain	$\langle n^{tr}\rangle$	$\langle n^{l}\rangle$	$\langle n^{t}\rangle$
Average size of	$\langle r^{tr}\rangle$	$\langle r^{l}\rangle$	$\langle r^{t}\rangle$
Probability of size r	$p^{tr}(r)$	$p^{l}(r)$	$p^{t}(r)$
Probability for n in an adsorbed chain	$P^{tr}(n)$	$P^{l}(n)$	$P^{t}(n)$

(relative) density of chains with their center of mass within 1.5 lattice layers from the surface is plotted vs chain length for two different surfaces (ϵ=0.0 and 1.0).

V. THE "ADSORBED" CHAIN

In this section we present our results on conformational features descriptive of the shape of chains at solid–melt interfaces. The use of the term "adsorbed chain," in the case of a pure polymer liquid, is merely an abbreviation for the more appropriate term "chains having at least one of their segments in contact with the surface." In general, an "adsorbed" chain has both "adsorbed" and free segments. Somewhat arbitrarily, only first layer segments were classified as "adsorbed." This choice was motivated by the weak surface effect on segment density and bond orientations inside the second layer (see Sec. III). Nonadsorbed segments are called "free."

Generally, an "adsorbed" chain consists of three types of segment sequences. These are sequences of adsorbed segments ("trains"), sequences of "free" segments connecting successive "trains" ("loops") and terminal sequences, which start at a "free" chain end and terminate just before the first (or last) "adsorbed" segment ("tails").

Knowledge of the average train, loop, and tail size and the average number of trains, loops, and tails per "adsorbed" chain, as well as, knowledge of the full statistical distribution of these quantities is of paramount importance in understanding chain dynamics. The various symbols used to designate these quantities are summarized in Table III.

A thorough study of all the above features was presented by Scheutjens and Fleer.[6] Their theory is, in some respects, a "mean field" theory (e.g., the Bragg–Williams approximation is used for the entropy of mixing inside each layer). Therefore, its predictions are expected to be most accurate at high densities. The simulation results contained in this subsection constitute a thorough test of the Scheutjens–Fleer theory predictions on chain conformations at the high density limit.

The Scheutjens–Fleer theory does not supply analytical expressions in the long chain limit, although fits of their numerical data suggest strongly the existence of certain power laws.[6] Scheutjens and Fleer comment quite often on the similarity between their high density predictions (melt) and those of Roe[12] for the single chain problem at a critical value of the surface–segment adsorption free-energy. Very insightfully, they attribute this similarity to the predominance of entropic factors in shaping chain conformations, which is common in both cases.

Based on the success of Silberberg's approach[8] in describing several other features of chain conformations (see Sec. IV) one would expect that analogous predictions on train, loop, and train features would also be accurate. However, such calculations were not presented in Silberberg's papers on solid–melt interfaces.[8] A few of the relevant calculations on train, loop, and tail features of random walks next to a reflective boundary were made (albeit in an incorrect context) in very early works related to the single chain problem.[39] The rest, which involve simple random walk statistics, are presented here. We derive of these results in order to show that one can arrive to quantitatively correct predictions of chain conformational statistics at solid–melt interfaces by using elementary "random walk" theory and quantifying only one "microscopic" parameter (number of chemical segments per Kuhn segment). All these calculations lead to predictions very similar to the single-chain at the critical absorption energy problem[10–13] and quantitatively very close to those of the Scheutjens–Fleer theory.[6]

Silberberg's rules for conformational swap between mirror image configurations do not affect either the size or the number of tails, trains, and loops. Therefore, the statistics of these entities may be studied *before* "reflection," inside an unconfined space, where the surface is replaced by an imaginary, *penetrable* plane.

The first step would be to enumerate the chain conformations, which encounter our penetrable plane. There are several ways to count these conformations. Here we present one which arrives at the final result in an expediting fashion, yet conceptually is not the most straightforward. Let N be the number of steps of a one-dimensional random walk in an unbounded space. We wish to count the number of N-step paths, which touch or cross a (penetrable) plane placed at 0. There are two types of such paths. Firstly, we have paths that start and terminate at 0. Their number is (Ref. 9),

$$N^{(0)}=\binom{N}{N/2}\simeq 2^N\left(\frac{2}{\pi N}\right)^{1/2}. \tag{5.1}$$

As we shall see later, this contribution, which is of order $2^N\partial(N^{-1/2})$, can be ignored. Second, we have the paths, which have at *most* one of their ends at 0. These N-step paths consist of an r-step tail and a $(N-r)$-step arbitrary path. Their number is (Ref. 9),

$$N_{(r)}^{(1,2)}=2^{(N+1-r)}\binom{r}{r/2}\simeq 2^{N+1}\left(\frac{2}{\pi r}\right)^{1/2}. \tag{5.2}$$

In the limit of large N, the total number of "adsorbed" paths will be

$$N^{\mathrm{ads}}=\int_0^N N^{(1,2)}(r)\,ds=2^{N+1}\left(\frac{2}{\pi}\right)^{1/2}N^{1/2}. \tag{5.3}$$

Note that N^0 was neglected, as it is of order $2^N\partial(N^{-1/2})$, while the error committed by passing to the continuous limit, is already of order $2^N\partial(1)$.

This prediction can be tested against our simulation results. It is convenient to think of our simulation system as being composed of two very wide half-films of width $h/2$ each (h is the simulation film-thickness). Then, the upper half of the film may be placed underneath the lower half and recreate in this way Silberberg's segregated chain groups. If indeed the statistical features of trains, loops, and tails are not affected by conformational swapping, and the resulting segregation of chains, the fraction of "adsorbed" chains in our simulation should be

$$f^{\mathrm{ads}}=\frac{2\left(\frac{2}{\pi}\right)^{1/2}\left[\frac{N-n^{\mathrm{tr}}}{3a_\infty}\right]^{1/2}}{h/2}, \tag{5.4}$$

where, $a_\infty=1.8$, the number of actual segments per Kuhn segment for our chains. The comparison between the predictions of Eq. (5.4) and simulation data are presented in Table IV. For $N>20$, it is quantitatively satisfactory, to say the least. Incidentally, Eq. (5.3) is a rederivation of an old result,[14] namely, that the configurational entropy loss of an ideal chain next to an *absorbing* barrier goes like $N^{1/2}$. The term n^{tr} in Eq. (5.4) appears for the following reason. For a one-dimensional random walk the train size is strictly zero (0 steps). Therefore, the one-dimensional random walk predictions are pertinent to three-dimensional chains of size, N^{eff},

$$N^{\mathrm{eff}}=N-n^{\mathrm{tr}}=3a_\infty N, \tag{5.5}$$

where n^{tr} is the number of segments in trains, as determined from our simulations.

TABLE IV. Fraction of adsorbed chains.

Chain length (N)	N^{eff} [Eq. (5.4)]	Adsorbed fraction [Eq. (5.5)]	Adsorbed fraction Simulation
5	2.0	0.10	0.17
10	5.6	0.17	0.23
20	13.5	0.24	0.28
30	21.8	0.21	0.23
50	39.8	0.17	0.18
100	83.7	0.21	0.20
200	177.5	0.30	0.28(±2)
300	274.0	0.38	0.36(±3)

We continue with features pertaining to chain tails. Among the N^{ads} adsorbed chain conformations $2^N(2/\pi N)^{1/2}$ have no tails while those with *exactly* one tail are $2^N[2-(2/\pi N)^{1/2}]$. The rest have two tails. Therefore, the fraction of chains with 0, 1, and 2 tails will be [see Eq. (5.3)]

$$P^t(0)=\tfrac{1}{2}N^{-1}, \tag{5.6a}$$

$$P^t(1)=\left(\frac{\pi}{2}\right)^{1/2}N^{-1/2}+\partial(N^{-1}), \tag{5.6b}$$

$$P^t(2)=1-\left(\frac{\pi}{2}\right)^{1/2}N^{-1/2}+\partial(N^{-1}). \tag{5.6c}$$

The average number of tails per adsorbed chain will be

$$\langle n^t\rangle=2-\left(\frac{\pi}{2}\right)^{1/2}N^{-1/2}+\partial(N^{-1}). \tag{5.7}$$

TABLE V. Average number of tails per adsorbed chain ($\langle n^t \rangle$) and average tail length ($\langle r^t \rangle$).

Chain length (N)	$\langle n^t \rangle$		$\langle r^t \rangle$			
	Eq. (5.7)	Simulation	Eq. (5.9) (leading term)	Eq. (5.9) (full)	Discrete random walk	Simulation
5	n/a	0.78	0.7	1.4	n/a	2.5
10	0.77	1.06	1.9	3.0	5.4	4.6
20	1.21	1.29	4.5	6.3	8.7	8.7
30	1.38	1.39	7.3	9.6	11.7	12.5
50	1.54	1.52	13.3	16.4	19.1	20(±2)
100	1.68	1.66	27.9	32.3	35.6	37(±4)
200	1.78	1.76	59.2	65.7	69.8	70(±7)
300	1.82	1.80	91.3	99.3	104.3	110(±12)

The comparison between the predictions of Eq. (5.7) and our simulation data are presented in Table V. For N$\geqslant$30 (or $N\geqslant 4$) the random walk next to a "reflective" surface prediction is virtually exact.

Let us consider now the distribution of tail sizes. From Eqs. (5.2), (5.3), and (5.7) we get in the continuous limit,

$$p^t(r)=\left[1+\frac{1}{2}\left(\frac{2}{\pi}\right)^{1/2}N^{-1/2}\right]\frac{r^{-1/2}}{N^{1/2}}. \tag{5.8}$$

The scaling is exactly that of a single chain next to a surface at the critical surface–segment adsorption free-energy.[12] Equation (5.8) also agrees closely with the long chain numerical data of the Scheutjens–Fleer theory at the high density limit.[6] Note that studies of the single chain problem[11–13] introduced a "stiffness parameter" in the partition function for trains. The power laws for single chains at the critical surface–segment free-energy exhibited a weak dependence on the value of this parameter. The prediction of Eq. (5.8), as well as predictions of the "reflective" boundary treatment on loops and trains, agree with the single chain predictions, when the "stiffness" correction factor is ignored. This is very satisfactory, as statistical segments, contrary to chemical segments, ought to be quite "flexible" entities.

In Fig. 8 we compare the predictions of Eq. (5.8) with simulation data. Two comments are in order. First, the correction term of $\partial(N^{-1/2})$ in the prefactor of Eq. (5.8) is quantitatively significant even for relatively long chains (N=100 or 200). This explains the slight difference between Roe's[12] asymptotic result for the single-chain at the critical adsorption free-energy (N/3) and the Scheutjens–Fleer prediction[2] for N=1000 (0.344 N). Second, our data for N=50 and 100 follow closely the prediction of the full expression in Eq. (5.8). On the other hand, the data follow a slope visibly different from $-\frac{1}{2}$ for very short chains (N =20). We think that even for N=20, this discrepancy originates mostly from our passing to the continuous limit, rather than the failure of random walk "reflective boundary" statistics. The effective cancellation of errors between the data and Eq. (5.8) provides some evidence for the above argument.

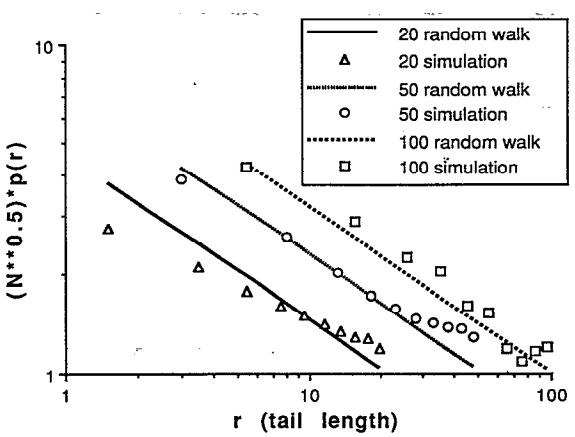

FIG. 8. Comparison between the random walk-reflective barrier prediction [Eq. (5.8)] and our data for the distribution of tail sizes.

The one-dimensional random walk next to a "reflective" surface has an average tail length

$$\langle r^t \rangle=\frac{1}{3}N+\frac{1}{6}\left(\frac{\pi}{2}\right)^{1/2}N^{1/2}. \tag{5.9}$$

The leading term is identical with Roe's single-chain prediction.[12] Table V compares our data on the average tail size with the long chain limit of Eq. (5.9), the full prediction of the same equation and values from an "exact" (i.e., discrete) random walk calculation. We see that the full prediction of Eq. (5.9) and the discrete random walk result agree quantitatively with our data for N$\geqslant$50 ($N>7$). The discrete random walk analysis leads to significantly improved predictions for very short chains (N<50).

We proceed with features pertaining to the number of adsorbed segment sequences ("trains"). Clearly, these quantities affect crucially the kinetics of chain "desorption," i.e., the mobility of chains at solid–melt interfaces. We consider an N-step one-dimensional random walk, which encounters the penetrable origin at 0, has a tail of length r, and subsequently *revisits* the origin n times. The probability of such a path is [Ref. 9, also see Eq. (5.3)],

$$p^{\mathrm{tr}}(n;s)=(2\pi Nr)^{-1/2}(N-r-n)^{-1/2}\times\exp[-n^2/2(N-r-n)]. \tag{5.10}$$

Anticipating that $n=\partial(N^{1/2})$, or more precisely, that for every r, $n=\partial(N-r)^{1/2}$, we may simplify Eq. (5.10) as follows:

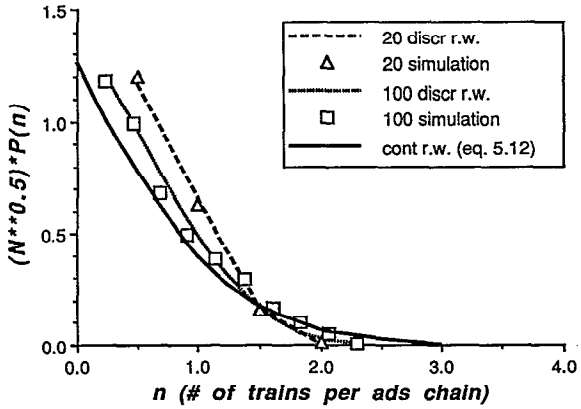

FIG. 9. Comparison between random walk-reflective barrier predictions [limiting form in Eq. (5.12) and discrete random walk] and our data for the distribution of the number of trains per adsorbed chain.

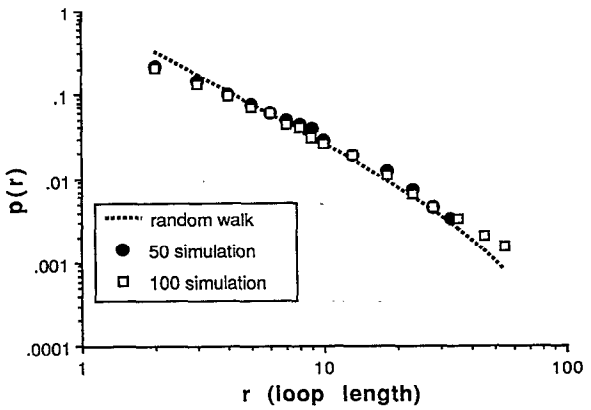

FIG. 10. Comparison between the random walk-reflective barrier prediction [Eq. (5.14)] and our data for the distribution of loop lengths.

$$P^{\mathrm{tr}}(n;s)\simeq(2\pi Nr)^{-1/2}(N-r)^{-1/2}\exp[-n^2/2(N-r)]. \tag{5.11}$$

Integrating over r we get the probability that an adsorbed chain has $n+1$ contacts ("trains") with the surface,

$$P^{\mathrm{tr}}(n+1)=(\pi/2N)^{1/2}\left[1-\frac{2}{\pi^{1/2}}\operatorname{erf}\left(\frac{n}{N^{1/2}}\right)\right]. \tag{5.12}$$

The prediction of Eq. (5.12) is compared against our simulation data in Fig. 9. It provides a semiquantitative approximation for N$\geqslant$50 ($N>7$). However, most of the discrepancy is the result of the error involved in passing from Eq. (5.10) to Eq. (5.11), i.e., the inequality $N>n^{\mathrm{tr}}$ is not strong enough for the chain lengths amenable to simulation study. When one compares the simulation data with the exact distribution resulting from Eq. (5.10), or even better its discrete random walk counterpart, the agreement is very satisfactory (Fig. 9).

Integrating Eq. (5.12) one gets for the average number of trains per adsorbed chain

$$\langle n^{\mathrm{tr}}\rangle=\frac{1}{2}\left(\frac{\pi}{2}\right)^{1/2}N^{1/2}. \tag{5.13}$$

The predictions of Eq. (5.13) are compared with our simulation data in Table VI. The agreement is satisfactory for N$>$20. Exact "random walk next to a reflective barrier" predictions agree with the simulation results, to within the statistical noise of the simulation data. Also, note that Roe's numerical prediction for the single chain problem[12] is 0.61 $N^{1/2}$, while that of Eq. (5.13) is 0.627 $N^{1/2}$.

We postpone our discussion on "train sizes" and their distribution until later. Instead we shift our focus to "loops." A loop is a sequence of "free" segments connecting successive "trains." Obviously, every adsorbed chain has a number of "loops" equal to its number of trains minus one. The probability of a "loop" of size r in an N-step one-dimensional random walk is [Ref. 9, see also Eqs. (5.2) and (5.13)] is

$$p^{l}(r)=(2\pi)^{-1/2}[r^{-3/2}-N^{-1}r^{-1/2}]. \tag{5.14}$$

The predictions of Eq. (5.14) are compared with our simulation data in Fig. 10. In spite of the passage to the continuous limit, and the approximations involved in Eq. (5.13) for the average number of "trains" per chain, the agreement is good and improves with chain length. This underscores the fact that "loops" are long [$\partial(N^{1/2})$] in the melt.

The average number of segments per loop result from integrating Eq. (5.14),

$$\langle r^{l}\rangle=\frac{2}{3}\left(\frac{2}{\pi}\right)^{1/2}N^{1/2}. \tag{5.15}$$

TABLE VI. Average number of trains per adsorbed chain ($\langle n^{\mathrm{tr}}\rangle$) and average train length ($\langle r^{\mathrm{tr}}\rangle$) and average loop length ($\langle r^{l}\rangle$).

Chain length (N)	$\langle r^{l}\rangle$		$\langle r^{\mathrm{tr}}\rangle$	$\langle n^{\mathrm{tr}}\rangle$		
	Eq. (5.15)	Simulation	simulation	Eq. (5.13)	Discrete random walk	Simulation
5	1.75	2.2	2.81	0.54	n/a	1.06(±3)
10	2.92	3.3	3.64	0.81	n/a	1.20(±3)
20	4.54	4.8	4.33	1.18	1.42	1.50(±5)
30	5.88	5.9	4.69	1.45	1.66	1.73(±5)
50	7.80	8.2(±1)	4.87	1.89	2.07	2.11(±8)
100	11.31	11.0(±3)	5.09	2.69	2.83	3.1(±2)
200	16.46	16.4(±5)	5.23	3.81	3.92	4.3(±4)
300	20.45	19(±1)	5.31	4.67	4.76	5.1(±8)

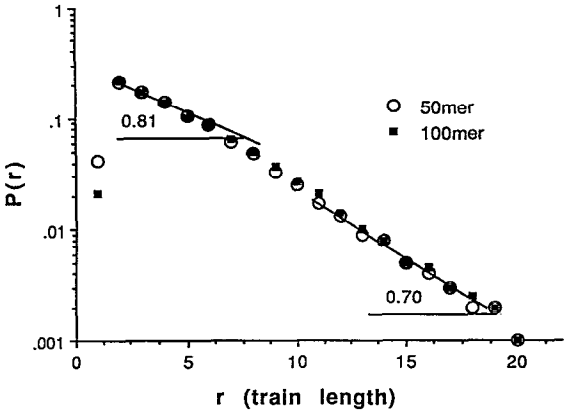

FIG. 11. Train size distributions for $N=50$ and 100, as determined from the simulations.

The continuous limit is quite satisfactory, as it reproduces quantitatively our simulation data (Table VI).

We would like to close this section by a discussion of average "train" sizes and "train" size distributions. A "train" of a three-dimensional random walk, which is unbounded in two dimensions and faces a "reflective" boundary in the third dimension is a generalization of the "contact" of a one-dimensional walk next to a "reflective" origin. Distribution of "train" sizes and the average "train" size are material specific. Their prediction lies outside the capabilities of the simple one-dimensional random walk analysis. Nevertheless, their study elucidates important aspects of the relevant physics.

The "train" size distribution determined from our simulations for $N=50$ and 100 is plotted in Fig. 11. As we can see, it is virtually independent of chain length (at least for $N>50$). Again this finding is in accordance with the single chain at the critical adsorption free-energy[11–13] and the Scheutjens–Fleer[6] predictions. It is also consistent with the spirit of the random walk next to a reflective boundary analysis.[8]

However, more interesting is the change of slope in Fig. 11. The tangent for short trains has a slope of 0.81 (± 0.01). This means a probability of 0.81 for stepping parallel to the surface, which is statistically identical with Helfand's prediction (0.815).[4] This slope, which indicates a preferential alignment parallel to the surface, reflects trends induced by the free energy minimization of *statistical* segments, that touch the surface. It represents therefore, the cubic lattice analog of a generic tendency, which would lead to flat conformations of *statistical segments* in contact with the surface. On the scale of our analysis it is a "microscopic" phenomenon.

The final slope in Fig. 11 is distinctly different from the initial slope. It is 0.70 (± 0.02), which is very close to $\frac{2}{3}$, the slope expected from (self-avoiding) random walks next to a fictitious, penetrable plane. Therefore, it constitutes an interesting microscopic demonstration of the inevitability of "reflection principle" statistics in the melt.

The chain length dependence of the average "train" *size* can be seen in Table VI. It is clear that the typical train has a size, which is chain length independent for long chains. Once more, this is in agreement with related,[6] and not so obviously related,[11–13] predictions. It is very tempting to identify the asymptotic average "train" length, which is very close to 5.4, with the reoccurring throughout this paper factor of 5.4 relating one-dimensional random walks to three-dimensional cubic lattice chains in the melt. This supports the claim that chain conformational statistics at solid–polymer melt interfaces, (on a scale larger than the statistical segment size), can be *quantitatively* predicted from simple random walk analysis and the knowledge of one "microscopic" quantity, the number of chemical segments per Kuhn segment (a_∞).

VI. SUMMARY

In this paper we have presented a comprehensive molecular simulation study of *long* chain conformational features at solid–melt interfaces. Our simulations examined the effect of surface–segment attraction at high densities, characteristic of polymer melts. As expected, surface–segment attraction produced only minor and very short range density variations. Furthermore, it did not have any observable effect on the bond orientational distribution, in agreement with relevant theoretical predictions.[4,7] These results quantified the proximity of melt systems with low compressibility to the zero compressibility (full-occupancy) limit, and underscored the "universality" of interfacial features.

Our data on chain conformations (chain dimensions, chain center of mass profiles, tail, loop and train length and number) confirmed fully the predictions of the Scheutjens–Fleer theory.[6] They also tested and confirmed the hypothesis on the similarity between chains at solid–melt interfaces and a single chain in a θ-solvent at the critical value of the adsorption free energy parameter.[10–13]

We performed extensive comparisons between the data from our computer experiments and predictions based on simple one-dimensional random walk next to a "reflective" barrier model. This model was introduced by Silberberg.[8] It suffers from difficulties caused by its ad hoc nature, but it has the important quality of furnishing simple analytical expressions for chain conformational features. Silberberg's predictions on the "adsorbed" amount, chain "start" profiles, center of mass profiles and chain dimensions were confirmed by our simulation data. Other predictions of the same approach on tails, loops, and trains were also in agreement with our simulation findings.

From a "material design" point of view, our work singled out the material-specific, "microscopic" parameters needed for a quantitative prediction of chain conformational features at solid–melt interfaces. It turned out that the knowledge of one such parameter, the number of chemical segments per statistical (Kuhn) segment (a_∞), suffices for a *quantitative* determination of all conformational features of "adsorbed" chains.

The simulation data supported this conclusion very strongly. The literal application of discrete one-dimensional random walk statistics, along with the knowledge of a_∞, predicted quite accurately all simulation results for chains longer than 6 (2 in one-dimension)

statistical segments. Clearly, these statistics describe not only the long chain limit, but the transition to it, as well. They become inappropriate only for *very* short chains (e.g., of molecular weight less than 400–500 for polyethylene), where segmental and chain length scales are *very* close.

All the above comments do not intend to undermine the value of a truly microscopic theory for solid–polymer melt interfaces. On the contrary, we believe that our studies, which illustrate the mechanisms by which segmental scale details influence chain scale features, have the potential to aid and complement genuinely microscopic analyses. There are many properties, crucial to material design (e.g., equation of state data), whose predictions are beyond the capabilities (and outside the scope) of the random-walk next to a "reflective barrier" approach supported by our simulation data. More importantly, a_∞ is a material property, whose *a priori* determination can only be furnished by such "microscopic," (i.e., segmental scale) theories. Perhaps, the link between segmental scale theories and phenomenological approaches is the "statistical segment partition function," or more precisely the ratio of this quantity inside the interface over that in the bulk. A microscopic theory would predict this quantity and estimate the error involved in successive renormalization iterations.

A simple and reliable predictive tool of chain conformations constitutes the structural background necessary for the analysis of chain dynamics. "Desorption" kinetics, chain mobility, and chain relaxation at solid–melt interfaces are much less "universal" than their static counterparts. In fact, they are profoundly "material specific," as our ongoing studies have shown.[38] A predictive capability of chain conformational features is a prerequisite, albeit not a sufficient condition, for understanding and utilizing this material specificity.

ACKNOWLEDGMENTS

During its early stages this work was supported by IBM through a S.U.R. grant with the University of Florida. For the past 12 months support was provided by NSF (Grant. No. CTS-9015882). I.A.B. would like to thank the Northeast Regional Data Center at the University of Florida for a significant allocation of computer through the Research Computing Initiative.

[1] A. Silberberg, J. Chem. Phys. **48**, 2835 (1968).
[2] C. A. J. Hoeve, J. Polym. Sci. **30**, 361 (1970); **34**, 1 (1971).
[3] R. J. Roe, J. Chem. Phys. **60**, 4192 (1974).
[4] E. Helfand, Macromolecules **9**, 307 (1976); T. A. Weber and E. Helfand, *ibid.* **9**, 311 (1976).
[5] E. A. DiMarzio and R. J. Rubin, J. Chem. Phys. **55**, 4318 (1971).
[6] J. M. H. M. Scheutjens and G. J. Fleer, J. Phys. Chem. **83**, 1619 (1979); **84**, 178 (1980); Macromolecules **18**, 1882 (1985).
[7] D. N. Theodorou, Macromolecules **21**, 1391 (1988); **21**, 1400 (1988).
[8] A. Silberberg, J. Colloid Interface Sci. **90**, 86 (1981); **125**, 14 (1988).
[9] W. Feller, *An Introduction to Probability and Its Applications* 3rd ed. (Wiley, New York, 1968), Vol. I, Chap. 3.
[10] C. A. J. Hoeve, E. A. DiMarzio, and P. Peyser, J. Chem. Phys. **42**, 2558 (1965).
[11] C. A. J. Hoeve, J. Chem. Phys. **43**, 3007 (1965).
[12] R. J. Roe, J. Chem. Phys. **43**, 1591 (1965); **44**, 4264 (1966).
[13] A. Silberberg, J. Chem. Phys. **46**, 1105 (1967).
[14] E. A. DiMarzio, J. Chem. Phys. **42**, 2101 (1965).
[15] G. ten Brinke, D. Ausserre, and G. Hadziioannou, J. Chem. Phys. **89**, 4374 (1988).
[16] K. F. Mansfield and D. N. Theodorou, Macromolecules **22**, 3143 (1989).
[17] S. K. Kumar, M. Vacatello, and D. Y. Yoon, J. Chem. Phys. **89**, 5206 (1988); Macromolecules **23**, 2189 (1990).
[18] I. Bitsanis and G. Hadziioannou, J. Chem. Phys. **92**, 3827 (1990).
[19] A. Yethiraj and C. K. Hall, Macromolecules **23**, 1865 (1990).
[20] M. Vacatello, D. Y. Yoon, and B. C. Laskowski, J. Chem. Phys. **93**, 779 (1990).
[21] M. W. Bivarsky and U. Landman, J. Chem. Phys. **97**, 1937 (1992).
[22] J. N. Israelachvili and S. J. Kott, J. Chem. Phys. **88**, 7162 (1988).
[23] J. P. Montfort and G. Hadziioannou, J. Chem. Phys. **88**, 7187 (1988).
[24] R. G. Horn, S. J. Hirz, G. Hadziioannou, C. W. Frank, and J. M. Catala, J. Chem. Phys. **90**, 6767 (1989).
[25] A. Kolinski, J. Scolnick, and R. Yaris, J. Chem. Phys. **84**, 1922 (1986).
[26] M. T. Gurler, C. C. Crabb, D. M. Dahlin, and J. Kovac, Macromolecules **16**, 398 (1982).
[27] F. T. Wall and F. Mandel, J. Chem. Phys. **63**, 4692 (1975).
[28] M. Lax and C. Brender, J. Chem. Phys. **67**, 1785 (1977).
[29] J. J. de Pablo and J. M. Prausnitz, Fluid Phase Equilibria **53**, 177 (1989).
[30] C. G. A. M. Mooij and D. Frenkel, Mol. Phys. **74**, 41 (1991).
[31] S. K. Kumar, I. Szliefer, and A. Z. Panagiotopoulos, Phys. Rev. Lett. **66**, 2935 (1991).
[32] D. A. McQuarrie, *Statistical Mechanics* (Harper and Row, New York, 1973).
[33] A. Yethiraj and C. K. Hall, Mol. Phys. **73**, 503 (1991).
[34] W. van Megen and I. Snook, J. Chem. Soc. Faraday Trans. II **75**, 1095 (1979); I. Snook and W. van Megen, J. Chem. Phys. **72**, 2907 (1980).
[35] K. Kremer and G. S. Grest, J. Chem. Phys. **92**, 5057 (1990).
[36] T. Hesselink, J. Phys. Chem. **75**, 65 (1971).
[37] R. J. Gaylord and D. J. Lohse, J. Chem. Phys. **65**, 2779 (1976).
[38] I. Bitsanis, "Desorption Kinetics and Relaxation of Polymer Chains at Solid–Melt Interfaces" (in preparation).
[39] R. Simha, H. L. Frisch, and R. F. Frisch, J. Phys. Chem. **57**, 584 (1953).